

# Effect of Chemically Reduced Graphene Oxide on Mechanical and Thermal Properties of Epoxy Nano Composites

Khan S, Bari P and Mishra S\*

Department of Plastics Technology, University Institute of Chemical Technology, Kavayitri Bahinabai Chaudhari North Maharashtra University, Jalgaon - 425001, Maharashtra, India

\*Corresponding author: Mishra S, Department of Plastics Technology, University Institute of Chemical Technology, Kavayitri Bahinabai Chaudhari North Maharashtra University, Jalgaon - 425001, Maharashtra, India, Tel: 9423488467, E-mail: profsm@rediffmail.com

Citation: Khan S, Bari P, Mishra S (2019) Effect of Chemically Reduced Graphene Oxide on Mechanical and Thermal Properties of Epoxy Nano Composites. J Mater Sci Nanotechnol 7(2): 203

Received Date: December 15, 2018 Accepted Date: August 05, 2019 Published Date: August 07, 2019

## Abstract

The reduced graphene oxide (rGO) was dispersed in ethanol using bath sonicator and mixed in 0.1,0.2,0.3,0.4 and 0.5 wt.% separately in the epoxy to make in situ composites by curing with diethylene triamine (DETA). The XRD and FE-SEM images confirmed intercalation and exfoliation as well as distribution patterns of rGO in epoxy. The carbon elemental mapping by EDX showed that the greater number of small void pockets in an ordered manner were present in 0.4 and 0.5 wt.% rGO/ epoxy composites in comparison to that of 0.2 and 0.3 wt. % composites. The mechanical properties increased with increase in rGO up to 0.3 wt. % due to the uniform dispersion of rGO up to 0.3 wt.% in epoxy. However, thermal properties did not show much improvement.

**Keywords:** Reduced Graphene Oxide; Epoxy; Mechanical properties; Thermal properties; EDX

## Introduction

Nowadays, inorganic nanofillers have proved their versatile applicability [1-6]. However graphene emerges as a rising star and new paradigms of relativistic condensed-matter physics and material science. The discovery of graphene is an important addition as a world's thinnest material due to its applications in drug delivery [7]. Energy production, photovoltaics [8,9], Fillers for polymer matrices [10-12], Sensors [13-16], electricals and electronics [17-20]. In recent year, there has been great interest in using graphene-based nanofillers, such as graphene sheets(GS) [21], Graphite nanoplate (GNPs) [22], Graphene oxide(GO) [23,24]. Now reduced graphene oxide (rGO) which gives new design of advance polymer nanocomposites [25]. Addition of 1 wt. rGO sheets in polyethylene matrix led to a 48% increment in the yield stress and 118% increment in the Young's modulus, respectively. However, the elongation at break decreased with increasing rGO sheets loading content [26].

Epoxy resin has been material of interest of the researchers for improvement in its properties by addition of less amount of nano particles [27-29]. Lee, *et al.* Prepared nanocomposites of epoxy resin and chemically reduced GO by thermal curing process and found an improvement in flexural strength and modulus of the epoxy nanocomposites by loading of rGO up to 0.4 wt. % compared to that of the neat - epoxy sheet [30]. Ganiu *et al.* prepared in situ thermally reduced graphene oxide/ epoxy composites [31]. They observed good dispersion of rGO and improvement in thermal conductivity and mechanical properties. A significant enhancement was observed in tensile, impact and flexural strength by the addition of 0.25 phr of microwave exfoliated reduced graphene oxide in epoxy nanocomposites cured by triethylenetetramine [28,32]. The Fe<sub>2</sub>O<sub>3</sub> decorated rGO in epoxy to improve the mechanical, thermal and electrical properties [33]. Jenkin, *et al.* dispersed the rGO in epoxy through combination of mechanical and sonication method followed by carbon fibre reinforcement in the composites [34]. They found that the composites' flexural strength and flexural modulus increased with rGO wt.% content up to 62% and 44% respectively the shear strength and modulus were also improved at maximum of 6% and 40% respectively. Zehao, *et al.* functionalized the GO with epoxy via esterification and prepared the CNT composites [35]. The functionalized GO effectively improves the dispersibility of CNTs in epoxy matrix due to good compatibility, which results in excellent mechanical properties of the hybrid structures. The improved interfacial interaction between 3D structure hybrids and epoxy matrix in fracture surface analysis indicated the covalent bonding formed between the epoxy molecular chain grafted on EGO and the hardener agent during the curing process.

In the present work the chemically reduced graphene was dispersed in the epoxy resin with diluent RD-113 and cured with Diethylene Triamine. The mechanical and thermal properties were determined. An attempt has also been made to correlate the dispersion of rGO in epoxy with EDX elemental mapping.

## Experimental

### Materials

Graphite powder (98%), from Lobel Chemical, Ortho-phosphoric acid ( $\text{H}_3\text{PO}_4$ , 85%) and Hydrogen Peroxide ( $\text{H}_2\text{O}_2$ , 30%) were purchased from Merck specialist Pvt. Ltd. Mumbai, India; Sulfuric acid ( $\text{H}_2\text{SO}_4$ , 97%), Potassium permanganate ( $\text{KMnO}_4$ , 99.9%), Petroleum Ether, Hydrazine Hydrate, Acetone and Ethanol (AR grade) were purchased from Rankem Thane, Maharashtra, India. Reactive diluents RD-113, Epoxy resin grade YD128 of EEW-189.5, viscosity 11,000-14,000 cp were procured from Aditya Birla Groups Mumbai, India. Curing agent Diethylene Triamine (DETA) was purchased from s. d. Fine. Chemicals Limited, Mumbai, India

**Synthesis of GO:** Graphite powder (3.0 g) was mixed into a solution of concentrated  $\text{H}_2\text{SO}_4$  and  $\text{H}_3\text{PO}_4$  at a 9:1 ratio (360:40 mL). Meanwhile, five to six times the weight of equivalent  $\text{KMnO}_4$  (18.0 g) powder was also added to graphite mixed solution. This reaction mixture was heated in a three-necked flask fitted with a water-cooled condenser having a temperature below 50 °C and allowed to stir continuously for 12 h. The reaction mixture was cooled to room temperature and then kept in an ice bath after the addition of 30%  $\text{H}_2\text{O}_2$ . The resulting suspension was filtered through polyester fiber cloth, and the remaining filtrate was centrifuged at 4000 rpm. The supernatant solution was decanted, and the residual solid material was washed with water, 30% HCl, and finally, ethanol. The solid material was coagulated with 200 mL of ether and vacuumdried overnight at room temperature.

**Synthesis of rGO:** Synthesized GO (900 mg) and distilled water (900 ml) were taken and sonicated for 30 min. Then the mixture was transferred into a round bottom flask and 9 ml hydrazine hydrate was added into the mixture. The mixture was kept for 24 h at 100 °C in an oil bath with mild stirring, allowed to settlement for 12 h and decanted. The decanted residue was washed with water and ethanol several times and filtered by using polyester cloth under vacuum filtration and dried for the whole night. In this manner several batches were carried out for rGO preparation from GO.

**Preparation of rGO/Epoxy Nanocomposite:** The Epoxy resin (83.23, 83.13, 83.03, 82.93 and 82.83 g) was taken separately and mixed with reactive diluents RD-113 (16.67 g). Acetone (10ml) as a solvent was also added in all samples to lower their viscosity. rGO (0.1, 0.2, 0.3, 0.4 and 0.5 g) was taken separately and mixed with ethanol (20ml) and sonicated in a bath sonicator for 30 min. The rGO solution was mixed into the respective resin samples under high speed for 45 min and kept at 80 °C in an oil bath till the solvent evaporation. This mixture was sonicated for 30 min and then 10 phr DETA was added to the mixture with stirring for a few seconds and poured the mixture into the mould. The mixture was degassed for 1 h and then cured at room temperature for 2-3 days. Samples were cut for mechanical and thermal testing.

### Characterization

**Tensile testing:** Tensile strength, young's modulus and elongation at break were performed on Universal Testing Machine (HI-TECH Instruments, Mumbai) at a cross-head speed of 50 mm min<sup>-1</sup>. The tensile tests were conducted according to ASTM D 638. The mean value of five samples is reported in the present work.

**Izod impact strength:** The izod impact tests were conducted on Izod Impact tester, (International Equipment's, Mumbai), by clamping a specimen vertically as a cantilever beam. The specimen is struck by the swing of pendulum released from a fix distance from the specimen clamp. The tests were repeated five times and average value is reported.

**Hardness:** The hardness tests were carried out by first placing a specimen on a hard and flat surface of Shore-D durometer. The pressure foot of the instrument was pressed onto the specimen, making sure that it was parallel to the surface of the specimen. The durometer hardness was read within 1 sec. After the pressure put was in firm contact with the specimen. The tests were repeated five times and mean values are shown as final results.

### Differential scanning calorimetry (DSC)

The differential scanning calorimetry was carried out on differential scanning calorimeter (model DSC60 SHIMADZU, Japan). A sample of 5-7 mg was sealed in aluminum pan and heated with the rate of 10 °C per min. Peak temperature and enthalpy ( $\Delta H$ ) were obtained from the maxima and the area of melting peak respectively.

**Thermo gravimetric analysis (TGA):** Thermo gravimetric analysis of the composites was conducted on TGA (model TGA- 50 SHIMADZU, Japan) by taking 5-7 mg of the sample with heating rate of 10 °C per min.

**Field emission scanning electron microscopy (FE-SEM):** Thermo The surface morphology of the fracture surfaces of the tensile specimens was examined by a scanning electron microscope (SEM, model S4800 type 2 HITACHI Japan) at 10 keV. The samples were coated with gold before analysis.

**X-ray diffraction (XRD):** XRD analysis of rGO/Epoxy was conducted on diffractometer (Advance X-ray diffractometer, D8, Bruker Germany) with  $\text{CuK}\alpha_1$  radiation ( $\lambda = 1.5404 \text{ \AA}$ ) within the  $2\theta$  range of 20-80°.

**Infrared spectroscopy:** Infrared spectroscopy was done on FTIR spectrophotometer (8400, Shimadzu, Japan) by dispersing samples of rGO and rGO epoxy composites in KBr powder. A total of 45 scans were taken for all of the composite samples; they were recorded at  $4000\text{--}400\text{ cm}^{-1}$  with a resolution of  $4\text{ cm}^{-1}$  in transmittance mode.

## Results and Discussion

### rGO Dispersion in Epoxy Composites

The rGO was treated with ethanol and dispersed into the epoxy matrix with acetone. The oxygen containing functional groups attached to the edges of the graphene sheet are responsible to allow the ethanol within the rGO sheets that results an increase in d spacing and ultimately smooth entrance of epoxy chains. The mechanism of dispersion of rGO in epoxy is illustrated in Figure 1. The proper dispersion of rGO into the matrix was studied with the help of XRD analysis (Figure 2). Figure 2 shows spectra of pristine epoxy and its composites. The broad curve between the region  $10^\circ$  to  $20^\circ$  is due to the scattering of epoxy molecule, indicating its amorphous nature [36]. The diffraction pattern found in 0.2 and 0.3 wt. % of rGO/Epoxy composites shows the same curve as the pristine epoxy, which indicate the good dispersion of rGO into the Epoxy matrix [36,37]. In 0.1, 0.4 and 0.5 wt. % composites, the diffraction pattern is disappeared; it indicates a good exfoliation of rGO into the epoxy matrix [36] (Figure 2).

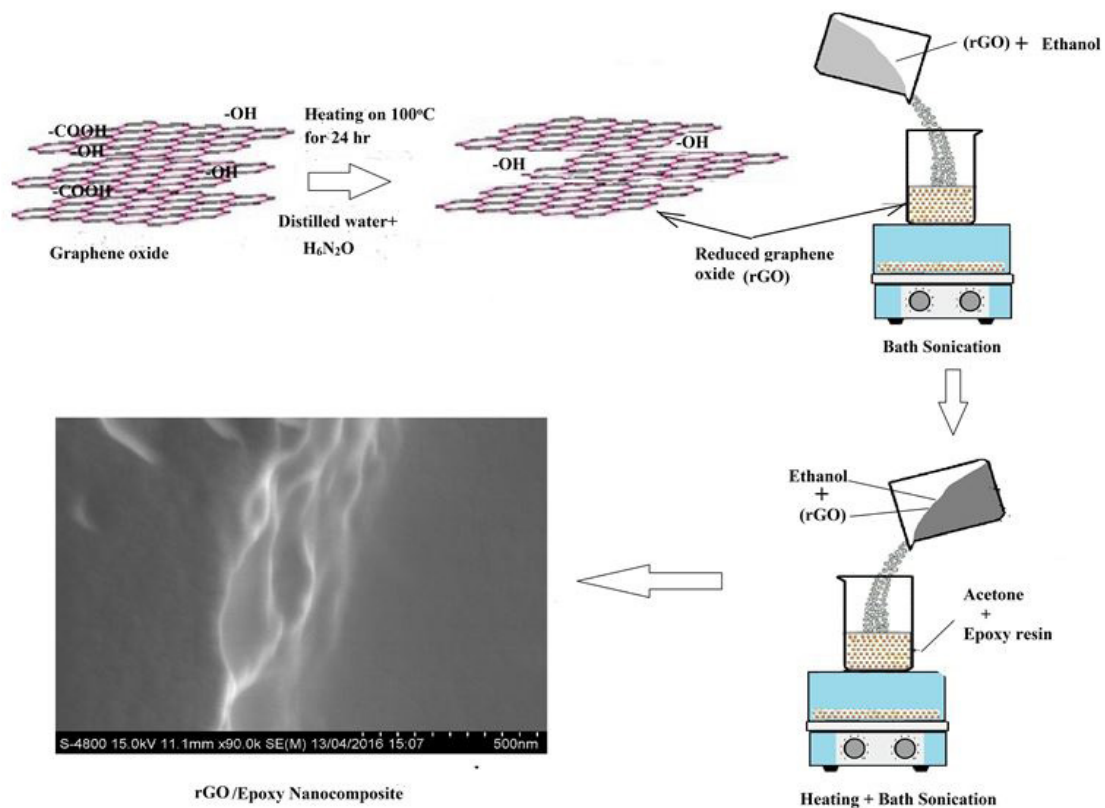


Fig.1. Schematic diagram of graphene oxide to rGO and epoxy / rGO composite

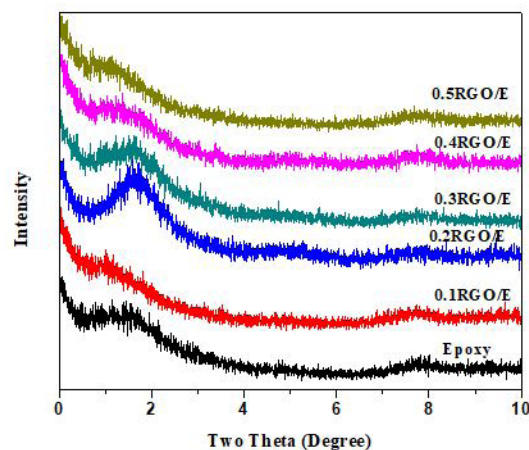


Fig.2. XRD patterns of rGO/epoxy composites



Figure 3 shows FESEM images of rGO and rGO/ Epoxy composites with different filler concentrations. Pristine epoxy sheet shows plane surface morphology (Figure 3b). In case of 0.2 and 0.3 wt. rGO/ Epoxy composites (Figure 3c and d), the proper dispersion of rGO is observed, While for 0.4 and 0.5 wt. rGO/Epoxy composites (Figure 3e and f), the exfoliation of rGO sheets is observed. To understand the dispersion behavior, the elemental mapping was done by EDX (Figure 4). Table given in Figure 4 shows the elemental contents of the different composites expressing greater carbon to oxygen ratio in 0.2 wt.% and 0.3 wt.% composites in comparison to that of 0.4 wt.% and 0.5 wt.%. It is clearly observed from Figure that the carbon distribution at 0.2 wt.% and 0.3 wt.% is very uniform except few regions, while 0.4 wt.% and 0.5 wt.% show uniform dispersion with greater number of bigger pockets throughout the spectra. This could be due to the exfoliation of rGO sheets (Figure 4).

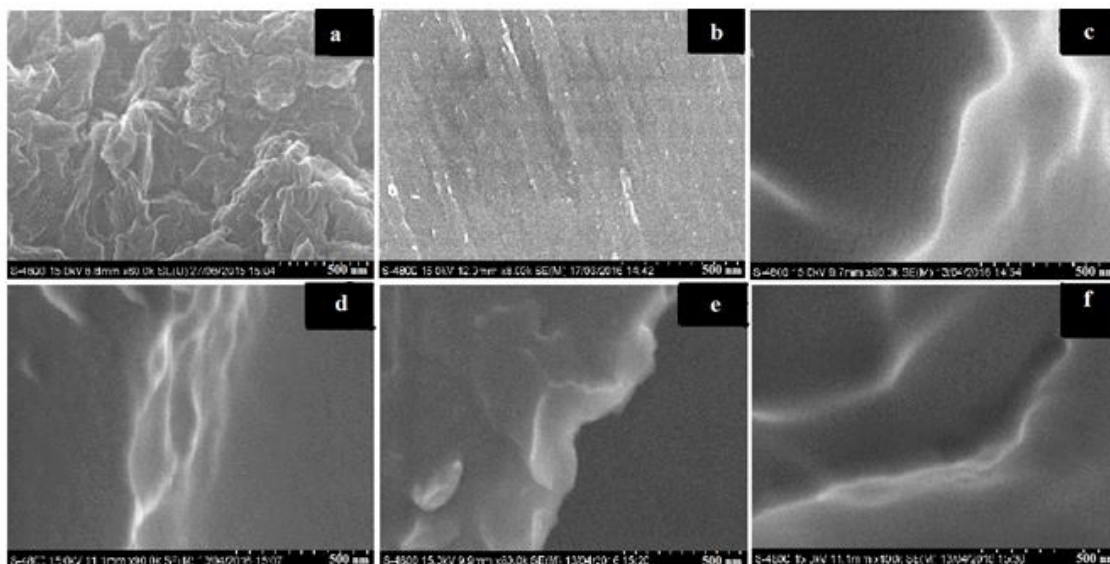


Fig.3. FE-SEM images of a) rGO; b) Epoxy; c) 0.2 wt.%; d) 0.3 wt.%; e) 0.4 wt.% and f) 0.5 wt.% rGO: epoxy composites

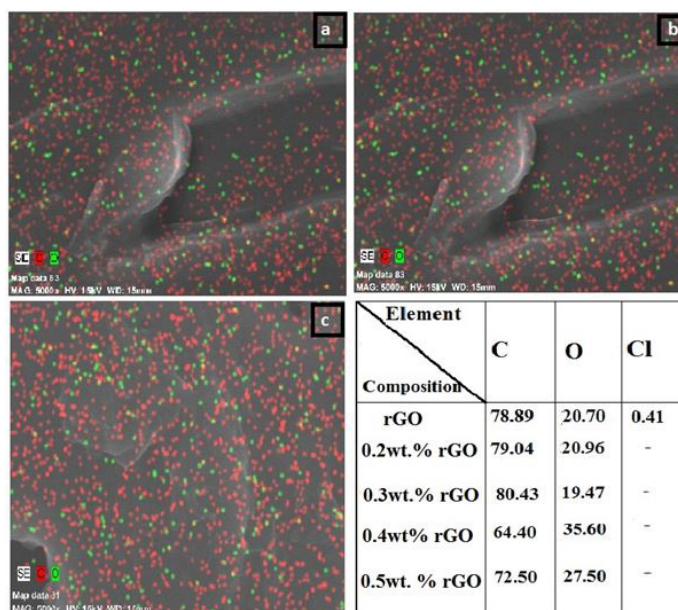


Fig.4. Carbon and Oxygen mapping of rGO : epoxy composites containing a) 0.2 wt. %; b) 0.3 wt.% and c) 0.5 wt.% rGO

### Mechanical Properties

The mechanical properties results illustrate that the tensile strength increases with increase in rGO content up to 0.3 wt.% (Figure 5). Maximum tensile strength (60 MPa) is obtained in composites filled 0.3 wt.% of rGO and minimum for 0.5 wt.% (32 MPa) which are greater than the virgin epoxy sheets (19 MPa).

Like tensile strength, the young’s modulus was also found to increase maximum up to 1217 MPa at 0.3 wt.% of rGO and minimum at 0.5 wt.% of rGO (493 MPa) in epoxy. However, virgin epoxy showed only 367 MPa (Figure 5). Thus the dimensional stability of the 0.3 wt.% filled composite is three times greater than the virgin epoxy. The maximum elongation (8.0 %) was observed for virgin epoxy. The minimum elongation (2.1%) is recorded at 0.3 wt. % addition of rGO. Further addition of rGO results in increment in elongation as recorded 4.5% for 0.5 wt. filled rGO composite (Figure 6).

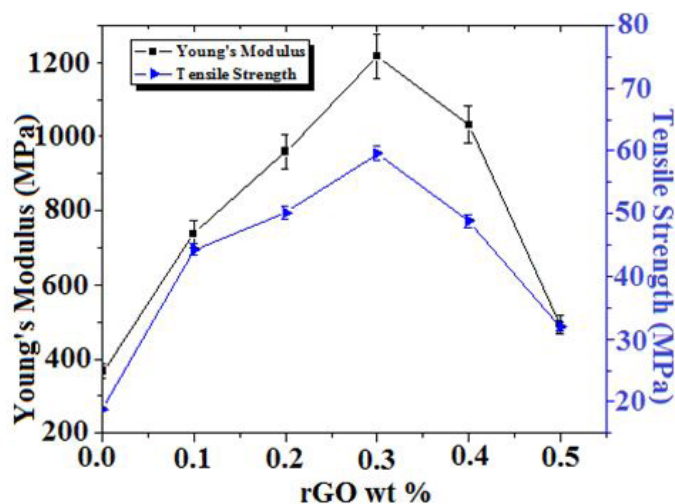


Fig.5. Tensile Strength and Young's Modulus of rGO/Epoxy composites

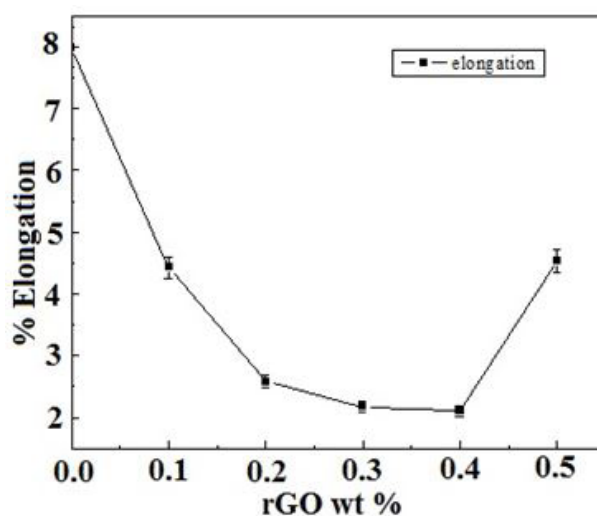


Fig.6. Elongation of rGO/Epoxy Composites at different wt.% of rGO

The impact strength and hardness of the composites are shown in Figure 7. The results of the impact strength were found to increase up to 0.3 wt.% addition of rGO in epoxy having the highest value as 126 J. The highest loading (0.5 wt.%) of rGO in epoxy showed only 117 J, which is less than the 0.3 wt.% filled rGO. On comprehensive comparison of the results, the epoxy without rGO had least (67 J) amongst all compositions; while 0.3 wt.% filled rGO composite showed approximately two times (126 J) improvement (Figure 7).

Like other mechanical properties, the hardness was also found to increase with increase in filler content up to 0.3 wt.% and decreased thereafter. The values of hardness were obtained as 75, 77, 81, 85, 82 and 81 for virgin epoxy, 0.1, 0.2, 0.3, 0.4 and 0.5 wt.% filled rGO composites respectively.

Thus the 0.3 wt. is the optimum amount to get maximum improvement in the mechanical properties. The reason behind improvement at 0.3 wt. is that the rGO sheets dispersed uniformly within the epoxy chains. As discussed earlier, the XRD patterns of the composites show very clear difference in 0.2 and 0.3 wt.% from other composites i.e. virgin epoxy, 0.1, 0.4 and 0.5 wt.% filled epoxy composites is due to the exfoliation of epoxy in rGO sheets (Figure 2). This exfoliation results in greater extent of cross linking by DETA in the epoxy chains. It is also observed from the FTIR spectra that the maximum peaks under the region of  $1650\text{ cm}^{-1}$  to  $2700\text{ cm}^{-1}$  have been eliminated in the 0.2 and 0.3 wt.% rGO/Epoxy composites in comparison to 0.1, 0.4 and 0.5 wt.% rGO/Epoxy composites (Figure 8). This is due to the elimination of C=O ( $1721\text{ cm}^{-1}$ ), C=C ( $1586\text{ cm}^{-1}$ ) and -OH ( $2701\text{ cm}^{-1}$ ) groups during crosslinking with epoxy matrix, which shows the proper dispersion of rGO into epoxy matrix. Higher level of improvement offered by rGO is attributed to the strong interaction of graphene sheets with epoxy because the covalent bonds between the carbon atoms of graphene sheets are much stronger than other layered nanomaterial such as silicon-based clay [38].

### Thermal properties

The DSC results illustrate that change in enthalpy increases with an increase in wt.% of rGO from 0.1 wt.% to 0.5 wt.%. However the least change in enthalpy was observed in virgin epoxy (Figure 9). These results show an increasing endothermic trend with

increasing amount of the filler. The results of thermogravimetric analysis indicate that there is very less difference in degradation of all composites for which onset is observed from 140 °C. However 0.3 wt.% rGO containing composite shows higher thermal stability amongst them; while cured virgin epoxy shows highest thermal stability depicting wt. loss from 350 °C onwards (Figure 10). The early wt. loss in rGO composites is due to the removal of moisture and remaining functional groups present on rGO.

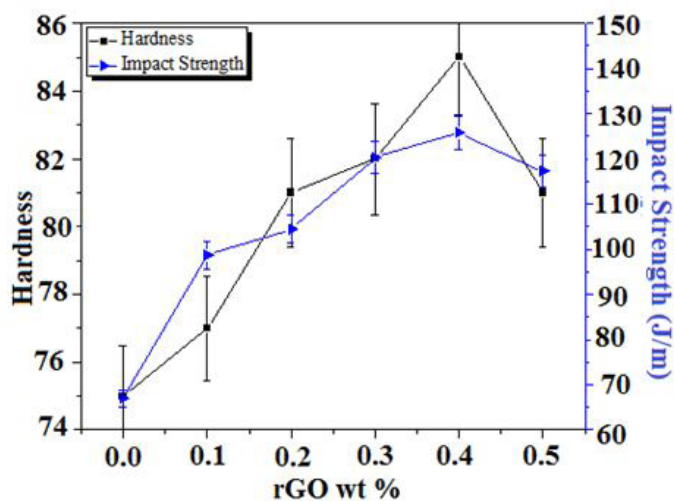


Fig.7. Impact Strength and Hardness of rGO/Epoxy Composites

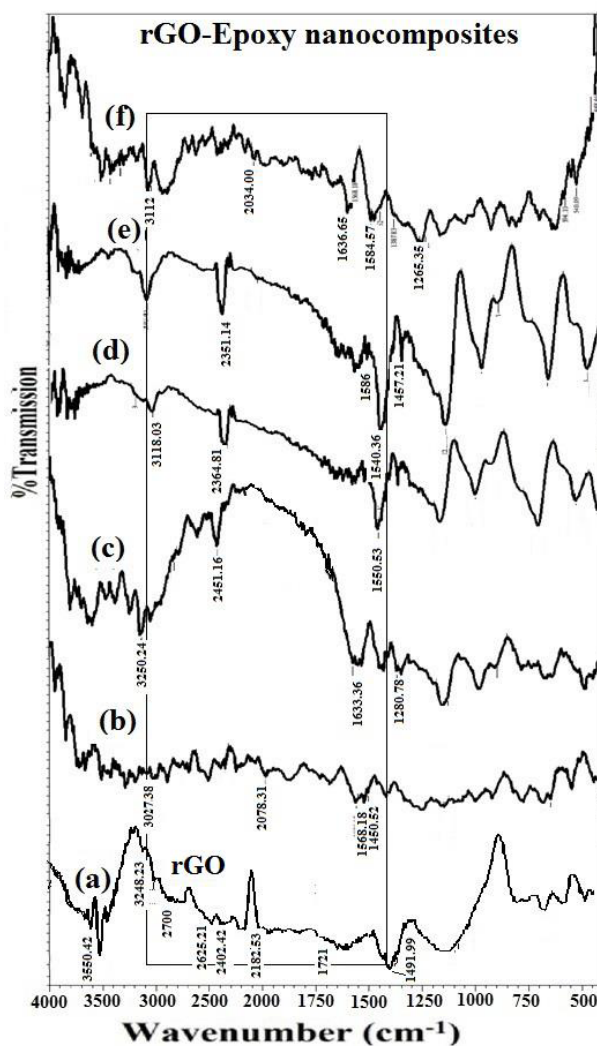


Fig.8. FTIR spectra of a) rGO ; b) 0.1wt.%; c) 0.2 wt.%; d) 0.3 wt.% ; e) 0.4 wt.% and f) 0.5 wt.% rGO: Epoxy composites

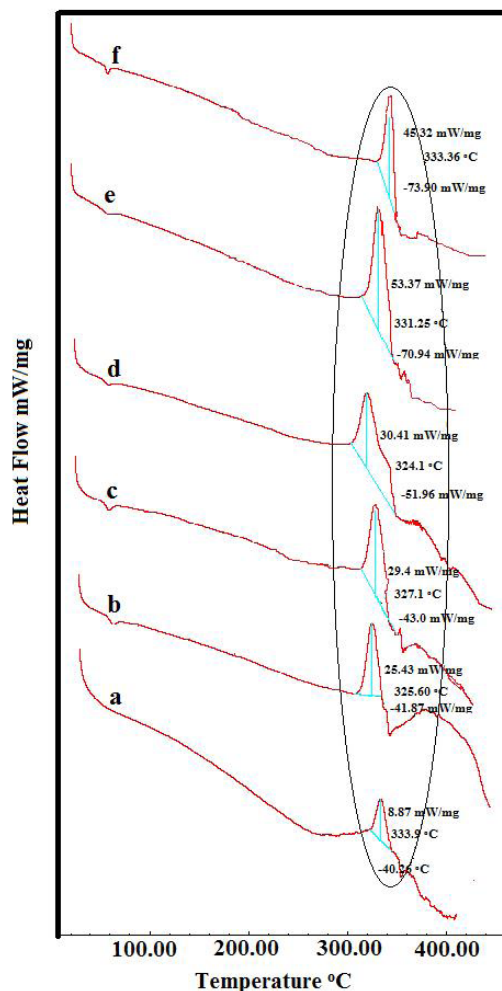


Fig.9. DSC analysis of a) virgin epoxy ; b) 0.1wt.% ; c) 0.2 wt.% ; d) 0.3 wt.% ; e) 0.4 wt.% and f) 0.5 wt.% rGO: Epoxy composites

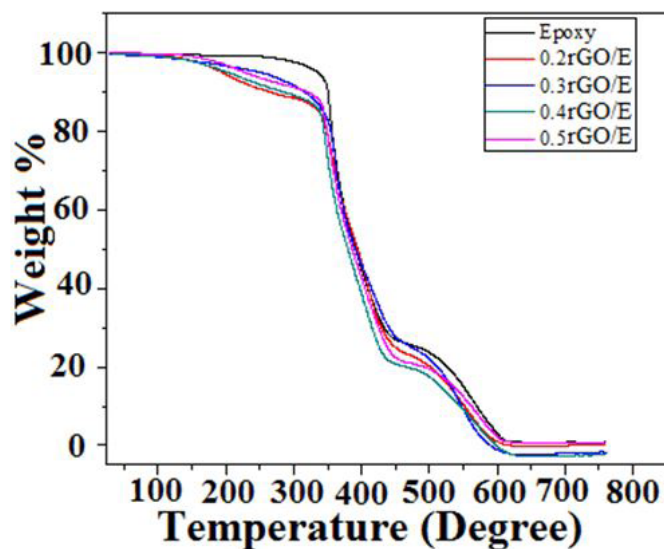


Fig.10. Thermogravimetric Analysis of epoxy : rGO composites

## Conclusion

Epoxy nano composites were prepared by reinforcing 0.1–0.5 wt.% of rGO dispersed with ethanol and bath sonicated before curing with diethylene triamine (DETA). There 0.2 wt.% and 0.3 wt.% additions result broad XRD peaks in the region of  $10^{\circ}$  to  $20^{\circ}$  due to intercalation of epoxy chains in rGO; while XRD grams of 0.4 and 0.5 wt.% do not show such peaks due to agglomeration (wrapping) of rGO sheets. These results are in agreement with FESEM images of the composites. The distribution of carbon and



oxygen measured by elemental mapping and change in carbon: oxygen ratio with increase in rGO from 0.2 wt.% to 0.5 wt.% also support the above results. More than two times improvement in tensile strength and young's modulus as well as increment in impact strength and hardness for 0.3 wt.% are remarkable achievements of the work. The thermal stability has also been improved of that wt.% in comparison to that of other composites.

## Acknowledgment

Authors are thankful to DST, Govt. of India and UKIERI, British Council for providing financial assistance (Project No. **DST/INT/UK/P-108/2014**) to carry out this research work.

## References

1. Patil SN, Paradeshi JS, Chaudhari PB, Mishra SJ, Chaudhari BL (2016) Bio-therapeutic potential and cytotoxicity assessment of pectin-mediated synthesized nanostructured cerium oxide. *Appl Biochem Biotechnol* 180: 638-54.
2. Sen T, Shimpi NG, Mishra S, Sharma R (2014) Polyaniline/ $\gamma$ -Fe<sub>2</sub>O<sub>3</sub> nanocomposite for room temperature LPG sensing. *Sens Actuators B: Chem* 190: 120-6.
3. Mishra S, Shimpi NG, Mali AD (2012) Investigation of photo-oxidative effect on morphology and degradation of mechanical and physical properties of nano CaCO<sub>3</sub> silicone rubber composites. *Polym Adv Technol* 23: 236-46.
4. Mishra S, Shimpi NG (2007) Studies on mechanical, thermal, and flame retarding properties of polybutadiene rubber (PBR) nanocomposites. *Polym Plast Technol Eng* 47: 72-81.
5. Chatterjee A, Khobragade PS, Mishra S (2015) Physicomechanical properties of wollastonite (CaSiO<sub>3</sub>)/styrene butadiene rubber (SBR) nanocomposites. *J Appl Polym Sci* 132.
6. Mishra S, Sonawane SS, Shimpi NG (2009) Influence of organo-montmorillonite on mechanical and rheological properties of polyamide nanocomposites. *Appl Clay Sci* 46: 222-5.
7. Rana VK, Choi MC, Kong JY, Kim GY, Kim MJ (2011) Synthesis and drug-delivery behavior of chitosan-functionalized graphene oxide hybrid nanosheets. *Macromolecular Materials and Engineering* 296: 131-40.
8. Cai W, Zhu Y, Li X, Piner RD, Ruoff RS (2009) Large area few-layer graphene/graphite films as transparent thin conducting electrodes. *Appl Phys Lett* 95: 123115.
9. Li X, Zhu Y, Cai W, Borysiak M, Han B, et al. (2009) Transfer of large-area graphene films for high-performance transparent conductive electrodes. *Nano Lett* 9: 4359-63.
10. Hansora DP, Shimpi NG, Mishra S (2015) Performance of hybrid nanostructured conductive cotton materials as wearable devices: an overview of materials, fabrication, properties and applications. *RSC Adv* 5: 107716-70.
11. Bari p, Lanjewar S, Hansora DP, Mishra S (2016) Influence of the coupling agent and graphene oxide on the thermal and mechanical behavior of tea dust – polypropylene composites. *J Appl Polym Sci* 133.
12. Hansora DP, Shimpi NG, Mishra S (2015) Graphite to graphene via graphene oxide: an overview on synthesis, properties, and applications. *JOM* 67: 2855-68.
13. Robinson JT, Perkins FK, Snow ES, Wei Z, Sheehan PE (2008) Reduced graphene oxide molecular sensors. *Nano Lett* 8: 3137-40.
14. Yeole B, Sen T, Hansora D, Mishra S (2016) Polypyrrole/metal sulphide hybrid nanocomposites: synthesis, characterization and room temperature gas sensing properties. *Mater Res* 19: 999-1007.
15. Mahajan C, Chaudhari P, Mishra S (2018) RGO–MWCNT–ZnO based polypyrrole nanocomposite for ammonia gas sensing. *J Mater Sci Mater Electron* 29: 8039-48.
16. Shimpi NG, Hansora DP, Yadav R, Mishra S (2015) Performance of hybrid nanostructured conductive cotton threads as LPG sensor at ambient temperature: preparation and analysis. *RSC Adv* 5: 99253-69.
17. Jain R, Mishra S (2016) Electrical and electrochemical properties of graphene modulated through surface functionalization. *RSC Adv* 6: 27404-15.
18. Jain R, Sharma DK, Mishra S (2019) High-Performance Supercapacitor Electrode of HNO<sub>3</sub> Doped Polyaniline/Reduced Graphene Oxide Nanocomposites. *J Electron Mat* 1-9.
19. Chaudhari P, Chaudhari V, Mishra S (2016) Low temperature synthesis of mixed phase titania nanoparticles with high yield, its mechanism and enhanced photoactivity. *Mat Res* 19: 446-50.
20. Watson G, Starost K, Bari P, Faisal N, Mishra S, et al. (2017) Tensile and flexural properties of hybrid graphene oxide/epoxy carbon fibre reinforced composites. *IOP Conf Ser: Mater Sci Eng* 195.
21. Schniepp HC, Li JL, McAllister MJ, Sai H, Herrera-Alonso M, et al. (2006) Functionalized single graphene sheets derived from splitting graphite oxide. *J Phys Chem B* 110: 8535-9.
22. Wang F, Drzal LT, Qin Y, Huang Z (2015) Multifunctional graphene nanoplatelets/cellulose nanocrystals composite paper. *Compos Part B: Eng* 79: 521-9.
23. Dreyer DR, Park S, Bielawski CW, Ruoff RS (2010) The chemistry of graphene oxide. *Chem Soc Rev* 39: 228-40.
24. Bari P, Samrin Khan, Njuguna J, Mishra S (2017) Elaboration of properties of graphene oxide reinforced epoxy nanocomposites. *Int J Plast Technol* 21: 194-208.
25. Mishra S, Hansora DP (2017) *Graphene Nanomaterials: Fabrication, Properties, and Applications* (1st Edn) Taylor Francis, New York.
26. Cao Z, Song P, Fang Z, Xu Y, Zhang Y, et al. (2012) Physical wrapping of reduced graphene oxide sheets by polyethylene wax and its modification on the mechanical properties of polyethylene. *J Appl Polym Sci* 126: 1546-55.
27. Alexandre M, Dubois P (2000) Polymer-layered silicate nanocomposites: preparation, properties and uses of a new class of materials. *Mater Sci Eng : R: Rep* 28: 1-63.
28. Wang Z, Massam J, Pinnavaia TJ (2000) *Epoxy-Clay Nanocomposites. A Text Book of Polymer-Clay Nanocomposites*, John Wiley Sons, Chichester 127-149.
29. Shimpi NG, Kakade RU, Sonawane SS, Mali AD, Mishra S (2011) Influence of nano-inorganic particles on properties of epoxy nanocomposites. *Polym Plast Technol Eng* 50: 758-61.
30. Lee AY, Chong MH, Park M, Kim HY, Park SJ (2014) Effect of chemically reduced graphene oxide on epoxy nanocomposites for flexural behaviors. *Carbon Lett* 15: 67-70.



31. Olowojoba GB, Eslava S, Gutierrez ES, Kinloch AJ, Mattevi C, et al. (2016) In situ thermally reduced graphene oxide/epoxy composites: thermal and mechanical properties. *Appl Nanosci* 6: 1015-22.
32. Sharmila TB, Nair AB, Abraham BT, Beegum PS, Thachil ET (2014) Microwave exfoliated reduced graphene oxide epoxy nanocomposites for high performance applications. *Polym* 55: 3614-27.
33. Sharmila TB, Antony JV, Jayakrishnan MP, Beegum PS, Thachil ET (2016) Mechanical, thermal and dielectric properties of hybrid composites of epoxy and reduced graphene oxide/iron oxide. *Mater Des* 90: 66-75.
34. Jenkins P, Siddique S, Khan S, Usman A, Starost K, et al. (2019) Influence of reduced graphene oxide on epoxy/carbon fibre-reinforced hybrid composite: flexural and shear properties under varying temperature conditions. *Adv Eng Mater*.
35. Qi Z, Tan Y, Zhang Z, Gao L, Zhang C, et al. (2018) Synergistic effect of functionalized graphene oxide and carbon nanotube hybrids on mechanical properties of epoxy composites. *RSC Adv* 8: 38689-700.
36. Wan YJ, Tang LC, Gong LX, Yan D, Li YB, et al. (2014) Grafting of epoxy chains onto graphene oxide for epoxy composites with improved mechanical and thermal properties. *Carbon* 69: 467-80.
37. Ma WS, Wu L, Yang F, Wang SF (2014) Non-covalently modified reduced graphene oxide/polyurethane nanocomposites with good mechanical and thermal properties. *J Mater Sci* 49: 562-71.
38. Zaman I, Manshoor B, Khalid A, Meng Q, Araby S (2014) Interface modification of clay and graphene platelets reinforced epoxy nanocomposites: a comparative study. *J Mater Sci* 49: 5856-65.

Submit your next manuscript to Annex Publishers and benefit from:

- › Easy online submission process
- › Online article availability soon after acceptance for Publication
- › Open access: articles available free online
- › More accessibility of the articles to the readers/researchers within the field
- › Better discount on subsequent article submission

Submit your manuscript at

<http://www.annexpublishers.com/paper-submission.php>

- › Rapid peer review process